Magnetic structure of the metallic triangular antiferromagnet Ag_2NiO_2

2013 J. Phys.: Condens. Matter 25 286005

(http://iopscience.iop.org/0953-8984/25/28/286005)

J. Phys.: Condens. Matter **25** (2013) 286005 (6pp) doi:10.1088/0953-8984/25/28/286005

Magnetic structure of the metallic triangular antiferromagnet Ag_2NiO_2

Hiroshi Nozaki[1], Martin Månsson[2], Bertrand Roessli[2], Vladimir Pomjakushin[2], Kazuya Kamazawa[1,5], Yutaka Ikedo[1,6], Henry E Fischer[3], Thomas C Hansen[3], Hiroyuki Yoshida[4,7], Zenji Hiroi[4] and Jun Sugiyama[1]

[1] Toyota Central R & D Laboratories, Inc., 41-1 Yokomichi, Nagakute Aichi 480-1192, Japan
[2] Laboratory for Neutron Scattering, ETH Zürich and Paul Scherrer Institut, CH-5232 Villigen PSI, Switzerland
[3] Institut Laue–Langevin, 6 rue Jules Horowitz, BP 156, F-38042 Grenoble Cedex 9, France
[4] Institute for Solid State Physics, University of Tokyo, Kashiwa, Chiba 277-8581, Japan

E-mail: h-nozaki@mosk.tytlabs.co.jp

Received 16 April 2013, in final form 4 June 2013
Published 21 June 2013
Online at stacks.iop.org/JPhysCM/25/286005

Abstract
The magnetic structure of the metallic antiferromagnet Ag_2NiO_2 with the Néel temperature $T_N = 56$ K has been investigated by means of a neutron diffraction technique using a powder sample in the temperature range between 5 and 65 K. The antiferromagnetic (AF) diffraction peaks are clearly observed below T_N and can be indexed with the propagation vector $\boldsymbol{k} = (1, \frac{1}{3}, \frac{1}{2})$. Based on the results of both a representational analysis and a Rietveld refinement of the magnetic peaks, the AF spin structure is determined as an A-type AF structure with $\boldsymbol{m}_l = \boldsymbol{m}_0 \cos(2\pi \boldsymbol{k} \cdot \boldsymbol{l})$, where $\boldsymbol{m}_l$ is the moment at the lth Ni^{3+} site and $\boldsymbol{m}_0 = (0.31, 0, 0.65)\ \mu_B$ at 5 K.

(Some figures may appear in colour only in the online journal)

1. Introduction

Disilver nickel dioxide, Ag_2NiO_2, in which the Ni ions form a two-dimensional triangular lattice (2DTL) in the NiO_2 plane, was firstly synthesized by Schreyer and Jansen [1] and found to be an antiferromagnetic (AF) metal with the Néel temperature $T_N = 56$ K. Both the metallic and AF nature appear simultaneously down to 0.4 K below T_N. However, the coexistence of static AF order and metallic conductivity is a rare case in the Ni-based 2DTL system, because the static AF order tends to preserve the itinerancy of the d electrons of the Ni ions. In fact, $LiNiO_2$ and $NaNiO_2$ are known to be AF insulators, while $AgNiO_2$ exhibits an AF semimetallic behavior due to a charge ordering of the Ni ions [2, 3]. Note that the Ni^{3+} ions are in a low-spin state with a $t_{2g}^6 e_g^1$ ($S = \frac{1}{2}$) configuration in these compounds, because of a strong crystalline electric field splitting of the d orbitals in the NiO_6 octahedra. As a result, the layered nickel dioxides have been considered to be good candidates for an ideal half-filled 2DTL. Nevertheless, only Ag_2NiO_2 is likely to range outside of a common AF insulator category.

In the Ag_2NiO_2 lattice, the NiO_2 planes are stacked with ABCABC sequence along the c-axis (see figure 1(a)). Interestingly, x-ray absorption near edge structure (XANES) measurements have revealed that the Ni valence state is Ni^{3+} rather than Ni^{2+}, while the Ag valence state is $Ag^{0.5+}$ [1]. Therefore, the charge valence of Ag_2NiO_2 is neutralized by the alternating stack of the $[NiO_2]^-$ and $[Ag_2]^+$ plane. This is most likely to suggest a significant role of the quarter-filled Ag 5s band in electron transport. In other words, only the Ag_2 plane exhibit a metallic conductivity, while the NiO_2 plane

[5] Present address: Tokai Project Office, Comprehensive Research Organization for Science and Society (CROSS), IBARAKI Quantum Beam Research Center (IQBRC), 162-1 Shirakata, Tokai, Ibaraki 319-1106, Japan.
[6] Present address: Muon Science Laboratory, Institute of Materials Structure Science, KEK, 1-1 Oho, Tsukuba, Ibaraki 305-0801, Japan.
[7] Present address: Strongly Correlated Materials Group, National Institute for Materials Science, 1-1 Namiki, Ibaraki 305-0044, Japan.

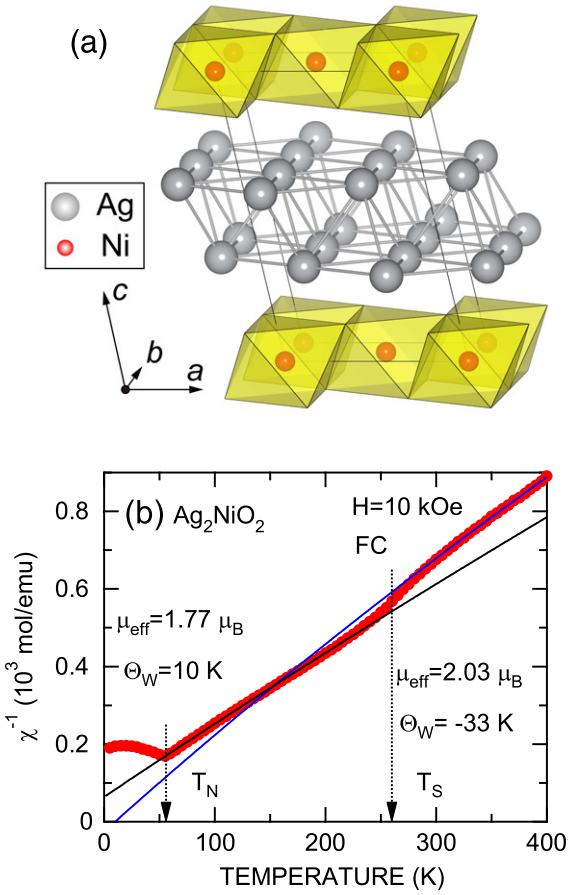

Figure 1. (a) Crystal structure of Ag_2NiO_2 with the space group $C2/m$ below T_s. The unit cell is indicated by the solid lines. (b) The temperature dependence of the inverse magnetic susceptibility under field cooled (FC) conditions [6]. The Weiss temperatures (Θ_w) and the effective magnetic moments (μ_{eff}) are obtained by Curie–Weiss fit in the temperature ranges 60–220 and 330–400 K. The values of $T_N = 56$ K and $T_s = 260$ K agree well with previous reports [1, 4].

is insulating due to AF order. This is the first scenario to explain the coexistence of AF order and metallic conductivity. However, in order to stabilize/complete long-range AF order, the interaction between the adjacent NiO_2 planes is expected to play a significant role. In addition, both resistivity (ρ) and heat capacity (C_p) measurements indicate the existence of two anomalies at $T_s = 260$ K and $T_N = 56$ K [4]. Recently, it was reported that Ag_2NiO_2 undergoes a structural change from a high-T rhombohedral phase to a low-T monoclinic phase with space group $C2/m$ at T_s, probably caused by the appearance of Jahn–Teller distortion of Ni^{3+}, but the details are still unknown [5].

Recent positive muon-spin rotation and relaxation (μ^+SR) measurements have supported the existence of two precession frequencies due to the presence of a static internal magnetic field (H_{int}) below T_N [6]. From the delay of the initial phase of the precession signal, the ground state of Ag_2NiO_2 was proposed to be an incommensurate spin density wave (IC-SDW) state, which is the second scenario for the coexistence of AF order and metallic conductivity [7, 8]. According to full potential first-principle calculations, the Ni ions are in a low-spin state with $S = \frac{1}{2}$ ($t_{2g}^6 e_g^1$) and are greatly affected by the Ag_2 layers [9]. Spin-polarized Hartree–Fock/DFT calculations predicted that the Ni ions are aligned ferromagnetically in the $[NiO_2]^-$ plane and coupled antiferromagnetically with the adjacent NiO_2 planes [5], i.e. A-type AF order, which is the third scenario for the coexistence of AF order and metallic conductivity, as in the case of $Na_{0.75}CoO_2$ [10, 11].

In order to clarify which scenario is reasonable for an explanation of the AF metallic nature of Ag_2NiO_2 and to further understand the role of the Ag_2 plane on the magnetism, it is crucial to determine the AF spin structure. Here, we therefore report the results of neutron diffraction measurements using a powder sample and magnetic structural analyses. As a result, the first scenario is found to be the most acceptable mechanism for the AF metallic nature.

2. Experimental details

A polycrystalline sample of Ag_2NiO_2 was synthesized at the University of Tokyo by a solid state reaction technique under an oxygen pressure of 65 MPa, using reagent grade Ag_2O and NiO powders as starting materials [4]. A powder x-ray diffraction (XRD) analysis showed that the sample was almost single phase of Ag_2NiO_2 ($R\bar{3}m$ with $a = 0.291$ nm, $c = 2.40$ nm at 297 K) with a small amount of unidentified phases. The amount of unidentified phases is estimated to be around 1% by the diffraction intensities. Initial neutron diffraction measurements were performed at the cold-neutron powder diffractometer DMC [12] at the Paul Scherrer Institut (PSI). However, because of the small size of the ordered magnetic moment, only the strongest AF Bragg peak could be measured with sufficient statistics. Therefore, in order to obtain more information about the magnetic structure of Ag_2NiO_2, more measurements had to be performed at the high-intensity two-axis diffractometer D20 [13] of the Institut Laue–Langevin (ILL), which provides the highest possible neutron flux. For the latter experiment the wavelength of the incident neutron beam was 0.2421 nm, which was monochromatized with pyrolytic graphite (002). The data were analyzed using the computer program FULLPROF [14].

3. Results

Figure 2 shows the neutron diffraction patterns acquired at 5 and 65 K at ILL. The calculated difference between the low- and high-temperature powder patterns is also plotted to show the pure magnetic diffraction peaks which are indicated by arrows. The magnetic peaks can be indexed with the propagation vector $\boldsymbol{k} = (1, \frac{1}{3}, \frac{1}{2})$ with the space group $C2/m$. The two peaks, which are not reasonably indexed by the same $\boldsymbol{k}$ vector, are also observed in the differential pattern at $2\theta = 44°$ and 60°. Since both the container and the cryostat produce no diffraction peaks at 44° and 60°, the two peaks are thought to originate from the powder sample. Therefore, the two peaks are most likely to come from a magnetic impurity phase that is also paramagnetic at 65 K. Unfortunately, it is very difficult, eventually impossible, to identify the impurity phase based

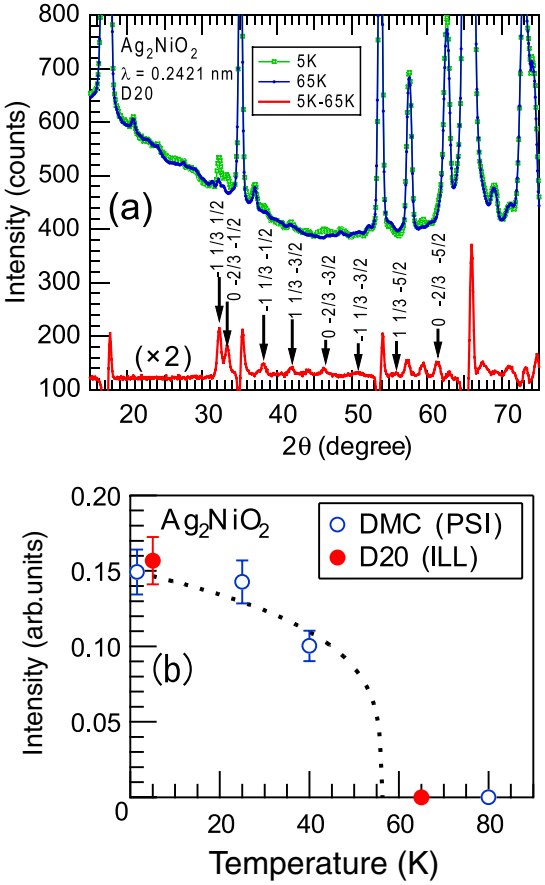

Figure 2. (a) Neutron diffraction patterns at 5 and 65 K, and the differential pattern between them. Magnetic Bragg peaks are indicated by arrows and indexed with the propagation vector $\boldsymbol{k} = (1, \frac{1}{3}, \frac{1}{2})$. There are two small peaks, which are not indexed, at around 44° and 60° in the differential pattern. (b) Temperature dependence of the 1 $\frac{1}{3}$ $\frac{1}{2}$ magnetic Bragg peak intensities, which are normalized to the main peak intensity. The dashed line is drawn for clarity.

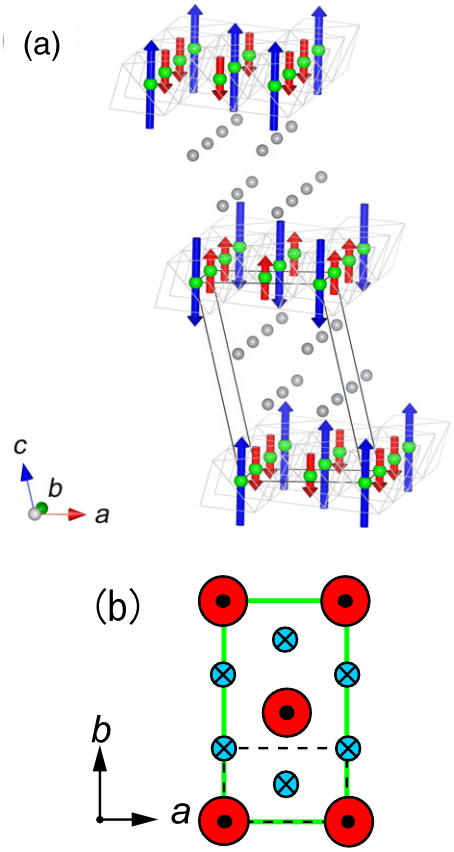

Figure 3. (a) A bird's-eye view of the magnetic structure corresponding to the possible irreducible representations of Γ_2 for the propagation vector $\boldsymbol{k} = (1, \frac{1}{3}, \frac{1}{2})$. Only Ni and Ag atoms are shown for clarity of display. The figures were generated with the computer program VESTA [36]. (b) The *ab*-plane of the Γ_2 structure, where the large and small circles correspond to the direction of Ni spins *in to* and *out of* the paper, respectively. Long (short) arrows and large (small) circles correspond to large (small) ordered Ni moment. The black dashed line and green solid line express the crystallographic and magnetic unit cells, respectively.

only on the two peaks. The presence of the impurity phase was also confirmed by XRD measurements. However, we wish to emphasize that the result of the magnetic structural analyses is not affected by the impurity phase, because the unidentified peaks are clearly distinguished from the magnetic Bragg peaks.

In order to obtain the possible magnetic structures for the Ni sublattices, we performed a symmetry analysis using the computer program BASIREPS [15]. For the propagation vector $\boldsymbol{k} = (1, \frac{1}{3}, \frac{1}{2})$ the decomposition of the possible magnetic structures in terms of the irreducible representations of the small group $G_{\boldsymbol{k}}$ is found as

$$\Gamma = \Gamma_1 + 2\Gamma_2. \tag{1}$$

Here, Γ_1 and Γ_2 correspond to the independent magnetic structures. Since $\boldsymbol{k} = (1, \frac{1}{3}, \frac{1}{2})$, the magnetic structure should be an amplitude modulated structure with a period of three unit cells along the *b*-axis and two unit cells along the *c*-axis. For the Γ_1 structure, the Ni moments are aligned parallel/antiparallel to the *b*-axis, but modulated along the [1 3 2]-direction. The Γ_2 structure also corresponds to the amplitude modulated structure, but with the moments aligned perpendicular to the NiO_2-plane. Figure 3 shows the Γ_2 AF model, in which there are two magnetically different Ni sites in the unit cell; that is, the magnitude of the ordered moment of one site is half of that of the other site. Note that all the Ni sites are crystallographically equivalent.

The results of a Rietveld refinement using the two models are shown in figure 4 and table 1. It is found that the Γ_2 structure provides a better fit to the experimental data; namely, the Bragg- and magnetic-*R* factors are $R_B = 1.66\%$ and $R_m = 26.5\%$, respectively, for the Γ_2 structure, whereas $R_B = 2.03\%$ and $R_m = 48.3\%$ for the Γ_1 structure. The magnetic moment $\boldsymbol{m}_l$ at the *l*th Ni site is described as

$$\boldsymbol{m}_l = \boldsymbol{m}_0 \cos(2\pi \boldsymbol{k} \cdot \boldsymbol{l}), \tag{2}$$

where $\boldsymbol{m}_0 = (0.31, 0, 0.65)\ \mu_B$ for the Γ_2 structure (see figure 3), as in the case of $BaCoO_3$. The magnitude of the ordered Ni moment, 0.67 μ_B, is almost one-third of the effective magnetic moment ($\mu_{eff} = 1.77\ \mu_B$), which was

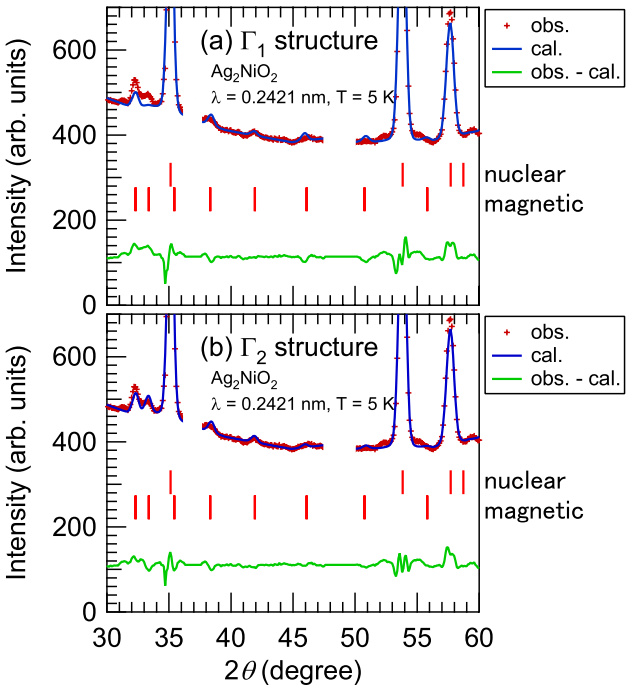

Figure 4. Rietveld refinement patterns for (a) the Γ_1 and (b) the Γ_2 structure. The two 2θ regions ($36.0° \leq 2\theta \leq 37.5°$ and $47.1° \leq 2\theta \leq 50.0°$) were excluded from the fit due to impurity peaks.

determined by a Curie–Weiss fit (see figure 1(a)) for the $\chi(T)$ curve in the T range between 60 and 220 K (above T_N).

4. Discussion

There are too many compounds represented by AMO_2, in which the M ions form a two-dimensional triangular lattice, to discuss their whole nature in a single regular paper. We, therefore, concentrate on layered nickel dioxides, $ANiO_2$, and disilver transition-metal dioxides, Ag_2MO_2, in order to deduce the origin of the AF order in Ag_2NiO_2.

4.1. Ag_2NiO_2 and other layered Ni dioxides

When we look at the component with $\mu_{ord} = 0.67\ \mu_B$ ($0.33\ \mu_B$), i.e. the long-blue (short-red) arrows in figure 3(b), each moment aligns parallel to another spin in the NiO_2 plane, but antiparallel to the spin in the adjacent NiO_2 planes, namely, the A-type AF order as in the case for $NaNiO_2$ [17–19]. Hence, the AF structure is thought to be a combination of the two A-type AF sublattices. Such a complex AF structure naturally increases the fluctuation of the Ni moments through the interaction between neighboring Ni moments in the NiO_2 plane. Furthermore, considering the projection to the *ab*-plane, the Ni ions in the adjacent NiO_2 planes are located at the center of the Ni triangular lattice due to the ABCABC stacking sequence along the *c*-axis. Since there are multiple pathways for the interaction with the Ni moments in the adjacent NiO_2 plane through the Ag_2 plane, the Ni moments are expected to be fluctuating along the *c*-axis.

Table 1. Results of the Rietveld refinement of the neutron powder diffraction data for Ag_2NiO_2 at 5 and 65 K (space group $C2/m$). The atomic positions are Ag(x, 0, z), Ni(0, 0, 0) and O(x, 0, z). R_{wp}, R_B and R_F represent the reliability (R)-factors for the whole pattern, Bragg and structure factor, respectively. The R-factors are sufficiently low, indicating that the analysis is well converged. The occupancies (g) for the Ag and O sites are variable, and are almost 100%.

Parameter		5 K	65 K
Ag	g	1.022(4)	1.022(4)
	x	0.217(2)	0.2125(1)
	z	0.6411(2)	0.6402(2)
O	g	1.009(5)	1.009(5)
	x	0.378(2)	0.378(2)
	z	0.1277(2)	0.1286(2)
Ni	g	1.0 (fixed)	1.0 (fixed)
a (nm)		0.504 21(3)	0.504 81(3)
b (nm)		0.291 54(2)	0.291 19(2)
c (nm)		0.818 49(3)	0.821 63(3)
β (°)		101.491(6)	102.246(5)
R_{wp} (%)		5.36	7.44
R_B (%)		1.68	4.63
R_F (%)		1.96	3.55

Concerning the discrepancy between the AF structure of Ag_2NiO_2 determined by neutron diffraction and that speculated by μ^+SR, we are still unable to find a correct reason. However, for the related compound, $LiCrO_2$ [20], in which the Cr^{3+} ions form a 2DTL, there are 36 magnetically different μ^+ sites in the lattice, when we assume the commensurate AF structure proposed by neutron. As a result, although the obtained zero field (ZF) μ^+SR spectrum below T_N consists of 36 precession signals with zero initial phase, the ZF-μ^+SR spectrum was well fitted by two precession signals with non-zero initial phase. That is, 48.6° and −52.7° at 1.7 K, as expected for an IC-SDW order. A similar explanation could be applicable for Ag_2NiO_2, due to the monoclinic distortion of the lattice below T_s.

Here, we wish to emphasize that the AF order for Ag_2NiO_2 is very different from that for $AgNiO_2$ [22, 23, 9, 2, 21, 3], which enters into an AF semimetallic phase below $T_N = 22$ K. This is because recent neutron work proposed that charge disproportionation of the Ni^{3+} ions ($3Ni^{3+} \rightarrow Ni^{2+} + 2Ni^{3.5+}$) occurs below T_N. The magnetic $Ni^{3.5+}$ ions are responsible for the AF order, while nonmagnetic Ni^{2+} ions still contribute semimetallic conductivity below T_N. The absence of charge disproportionation in Ag_2NiO_2 suggests that all the Ni^{3+} moments order antiferromagnetically below T_N, indicating that the NiO_2 plane is insulating. Therefore, the Ag_2 plane is found to be responsible for the metallic conductivity. This leads to a question on the origin of the AF interaction across the Ag_2 plane. For $NaNiO_2$ [24], the Ni–O–Na–O–Ni interaction via the empty 3s orbital of the Na ions plays an essential role to form A-type AF order with $T_N = 20$ K. However, it is most unlikely that a similar Ni–O–Ag–Ag–O–Ni interaction via the 5s orbital of Ag, which is quarter-filled, is responsible for the AF order of Ag_2NiO_2. This is because the T_N of Ag_2NiO_2 is 2.8 times

higher than the T_N of $NaNiO_2$, despite a large separation between the two adjacent NiO_2 planes, i.e. $c = 0.82$ nm for Ag_2NiO_2, whereas $c = 0.56$ nm for $NaNiO_2$.

We thus consider the other interaction through metallic Ag_2 planes. That is, the interlayer AF coupling between the adjacent NiO_2 layers could be induced by an RKKY-type interaction [25] via itinerant 5s electrons instead. This is consistent with the results of electronic structural calculations using a Hartree–Fock/DFT method, which show that the Ag 5s/5p bands cross the Fermi level [5]. The calculations predicted that AF order between the Ni moments in the adjacent NiO_2 planes is more stable than FM order [5], indicating the formation of A-type AF order. The same calculations also proposed the appearance of ferrimagnetic order in the NiO_2 plane, when FM electron correlation is decreased [5]. The proposed ferrimagnetic structure looks similar to the present neutron result, if we ignore the lack of an amplitude modulation in the calculated result. Since the T_N(=56 K) of Ag_2NiO_2 is higher than the T_N(=20 K) of $NaNiO_2$, the RKKY-like interlayer AF interaction via the 5s electrons of the Ag_2 plane is naturally stronger than the interlayer AF interaction of $NaNiO_2$. Such a strong AF interaction in Ag_2NiO_2 is expected to stabilize the ferrimagnetic order in the NiO_2 plane.

On the other hand, DFT calculations on $NaNiO_2$ suggest a weak FM interaction (∼1 meV) in the NiO_2 plane due to the 90° Ni–O–Ni exchange, while the interlayer AF interaction through the Ni–O–Na–O–Ni path is much weaker (∼0.1 meV) [26]. Now we discuss the magnetic order within the *ab*-plane. The arrangement of Ni moments in the *ab*-plane for Ag_2NiO_2 is similar to that for $CsCoBr_3$ [27, 28] and $BaCoO_3$ [16]. In $CsCoBr_3$, the inter-plane magnetic interaction is two orders of magnitude weaker than that within the *ab*-plane. The magnetic order in the *ab*-plane is due to the nearest-neighbor (J_1) and second-neighbor (J_2). Since $J_1 \sim -80$ K (−6 meV) and $J_2 \sim +0.8$ K (0.06 meV), the AF order is naturally formed in the *ab*-plane. $BaCoO_3$ shows the amplitude modulated AF structure although charge ordering does not appear. As in $CsCoBr_3$, the exchange interaction in the *ab*-plane is weaker than that along *c*-axis due to the large separation by Ba ions in the *ab*-plane. Nevertheless, 3D AF order is formed in $BaCoO_3$ as confirmed by neutron diffraction study [16]. Therefore, the AF order in the *ab*-plane is led by the Co–O–O–Co interaction. The shortened magnetic moment on the Ni ion compared with the other one is probably due to the fluctuation of the Ni moment, as discussed in $CsCoBr_3$ and $CsNiCl_3$ [27, 29]. As in the case of $CsCoBr_3$ and $BaCoO_3$, the AF order in the *ab*-plane in Ag_2NiO_2 is formed by the interaction in the NiO_2 plane with the comparably large inter-plane interaction.

4.2. Ag_2NiO_2 and other disilver metal dioxides

Besides Ag_2NiO_2, three other disilver transition-metal (M) dioxides were recently prepared using a solid state reaction technique under high-pressure, namely, Ag_2MnO_2 [30–32], Ag_2CrO_2 [33, 34], and Ag_2FeO_2 [35]. Although the detailed physical properties of Ag_2FeO_2 are still not clarified, the other two compounds are reported to exhibit metallic conductivity down to the lowest T measured. Furthermore, as T decreases from ambient T, Ag_2MnO_2 undergoes successive magnetic transitions from a Curie–Weiss paramagnetic phase with $\Theta_W = -370$ K to a short-range magnetic ordered phase at $T_N = 80$ K [31], and then to a spin-glass phase at $T_g = 22$ K [32]. In contrast, Ag_2CrO_2 is a Curie–Weiss paramagnet with $\Theta_W = -95$ K, and enters into a long-range partially disordered state with five sublattices below $T_N = 24$ K [34].

Here, we should note that the triangular lattices of Mn^{3+} and Cr^{3+} ions are distorted at low T in both compounds, resulting in isosceles triangular lattices. For Ag_2MnO_2, a Jahn–Teller distortion of each MnO_6 octahedron is thought to be responsible for the macroscopic structural distortion [34], but the mechanism of the distortion is still not clarified for Ag_2CrO_2. Anyway, such a structural distortion naturally enhances the anisotropic magnetic interaction in the MO_2 plane. This could be the reason for the absence of long-range AF order in Ag_2MnO_2 and Ag_2CrO_2. In contrast, the present neutron work indicates that this distortion is very small for Ag_2NiO_2 compared to those for Ag_2MnO_2 and Ag_2CrO_2; namely, the length of two edges of the Ni triangle is 0.291 21 nm and that of the bottom edge is 0.291 54 nm. The distortion (δ) is, hence, 1.001(=0.291 54/0.291 21) for Ag_2NiO_2, whereas $\delta = 0.971$ for Ag_2MnO_2 [32] and $\delta = 0.996$ for Ag_2CrO_2 [34].

Back to $NaNiO_2$, despite the fact that $\delta = 0.944$ due to a Jahn–Teller distortion of the Ni^{3+} ion, long-range AF order is established below $T_N = 20$ K [17, 18]. This suggests that, although the structural distortion is one of the parameters that determines the magnetic ground state of the triangular lattice, the electron configuration of the M^{3+} ion is also an important factor. In particular, an orbital degree of freedom of the e_g level is most likely predominant for the formation of long-range AF order.

5. Conclusion

Based on powder neutron diffraction measurements on the metallic triangular antiferromagnet Ag_2NiO_2 with $T_N = 56$ K, the AF structure has been determined as an amplitude modulated structure with propagation vector $\boldsymbol{k} = (1, \frac{1}{3}, \frac{1}{2})$. Although the magnetic NiO_2 planes are thought to be well spatially separated by the Ag_2 planes, the interaction between adjacent NiO_2 planes plays a significant role in forming the AF order along the *c*-axis, indicating the presence of a magnetic interaction path via the Ag_2 plane. Therefore, it is clarified that the Ag_2 plane is responsible for the metallic conductivity and is essential for the formation of long-range AF order on the NiO_2 plane through an RKKY-type 3d–5s interaction.

Acknowledgments

This work is in part based on experiments performed at Institut Laue–Langevin (ILL), Grenoble, France, as well as the Swiss spallation neutron source SINQ, Paul Scherrer Institut (PSI), Villigen, Switzerland. We thank the ILL/PSI

staff for help with the neutron scattering experiment. YI and JS are partially supported by the KEK–MSL Inter-University Program for Overseas Muon Facilities. A part of this work was also supported by Grant-in-Aid for Scientific Research on Innovative Areas 'Ultra Slow Muon' (No. 23108003), of the Ministry of Education, Culture, Sports, Science, and Technology, Japan.

References

[1] Schreyer M and Jansen M 2002 *Angew. Chem.* **41** 643
[2] Wawrzyńska E, Coldea R, Wheeler E M, Mazin I I, Johannes M D, Sörgel T, Jansen M, Ibberson R M and Radaelli P G 2007 *Phys. Rev. Lett.* **99** 157204
[3] Wawrzyńska E, Coldea R, Wheeler E M, Sörgel T, Jansen M, Ibberson R M, Radaelli P G and Koza M M 2008 *Phys. Rev.* B **77** 094439
[4] Yoshida H, Muraoka Y, Sörgel T, Jansen M and Hiroi Z 2006 *Phys. Rev.* B **73** 020408(R)
[5] Wedig U, Adler P, Nuss J, Modrow H and Jansen M 2006 *Solid State Sci.* **8** 753
[6] Sugiyama J, Ikedo Y, Mukai K, Brewer J H, Ansaldo E J, Morris G D, Chow K H, Yoshida H and Hiroi Z 2006 *Phys. Rev.* B **73** 224437
[7] Krishnamurthy H R, Jayaprakash C, Sarker S and Wenzel W 1990 *Phys. Rev. Lett.* **64** 950
[8] Fujita M, Ichimura M and Nakao K 1991 *J. Phys. Soc. Japan* **60** 2831
[9] Johannes M D, Streltsov S, Mazin I I and Khomskii D I 2007 *Phys. Rev.* B **75** 180404(R)
[10] Bayrakci S P, Mirebeau I, Bourges P, Sidis Y, Enderle M, Mesot J, Chen D P, Lin C T and Keimer B 2005 *Phys. Rev. Lett.* **94** 157205
[11] Helme L M, Boothroyd A T, Coldea R, Prabhakaran D, Tennant D A, Hiess A and Kulda J 2005 *Phys. Rev. Lett.* **94** 157206
[12] Fischer P and Keller L 2000 *Neutron News* **11** 19
[13] Hansen T C, Henry P F, Fischer H E, Torregrossa J and Convert P 2008 *Meas. Sci. Technol.* **19** 034001
[14] Rodriguez-Carvajal J 1993 *Physica* B **192** 55
[15] Rodriguez-Carvajal J 1991 *BASIREPS* www.ill.fr/sites/fullprof/php/downloads.html
Izyumov Y A *et al* 1991 *Neutron Diffraction of Magnetic Materials* (New York: Consultants Bureau)
[16] Nozaki H, Janoschek M, Roessli B, Sugiyama J, Keller L, Brewer J H, Ansaldo E J, Morris G D, Takami T and Ikuta H 2007 *Phys. Rev.* B **76** 014402
[17] Darie C, Bordet P, de Brion S, Holzapfel M, Isnard O, Lecchi A, Lorenzo J E and Suard E 2005 *Eur. Phys. J.* B **43** 159
[18] Lewis M J, Gaulin B D, Filion L, Kallin C, Berlinsky A J, Dabkowska H A, Qiu Y and Copley J R D 2005 *Phys. Rev.* B **72** 014408
[19] Baker P J, Lancaster T, Blundell S J, Brooks M L, Hayes W, Prabhakaran D and Pratt F L 2005 *Phys. Rev.* B **72** 104414
[20] Sugiyama J, Månsson M, Ikedo Y, Goko T, Mukai K, Andreica D, Amato A, Ariyoshi K and Ohzuku T 2009 *Phys. Rev.* B **79** 184411
[21] Lancaster T, Blundell S J, Baker P J, Brooks M L, Hayes W, Pratt F L, Coldea R, Sörgel T and Jansen M 2008 *Phys. Rev. Lett.* **100** 017206
[22] Shin Y J, Doumerc J P, Dordor P, Delmas C, Pouchard M and Hagenmuller P 1993 *J. Solid State Chem.* **107** 303
[23] Kikuchi H, Nagasawa H, Mekata M, Fudamoto Y, Kojima K M, Luke G M, Uemura Y J, Mamiya H and Naka T 1999 *Hyperfine Interact.* **120/121** 623
[24] Reitsma A J W, Feiner L F and Olés A M 2005 *New J. Phys.* **7** 121
[25] Ruderman M A and Kittel C 1954 *Phys. Rev.* **96** 99
Kasuya T 1956 *Prog. Theor. Phys.* **16** 45
Yoshida K 1957 *Phys. Rev.* **106** 893
[26] Meskine H and Satpathy S 2005 *Phys. Rev.* B **72** 224423
[27] Yelon W H, Cox D E and Eibschütz M 1975 *Phys. Rev.* B **12** 5007
[28] Todoroki N and Miyashita S 2004 *J. Phys. Soc. Japan* **73** 412
[29] Yelon W B and Cox D E 1972 *Phys. Rev.* B **7** 2024
[30] Yoshida H, Ahlert S, Jansen M, Okamoto Y, Yamaura J and Hiroi Z 2008 *J. Phys. Soc. Japan* **77** 074719
[31] Sugiyama J, Nozaki H, Ikedo Y, Mukai K, Russo P L, Andreica D, Amato A, Yoshida H and Hiroi Z 2008 *Phys. Rev.* B **78** 104427
[32] Ji S *et al* 2010 *Phys. Rev.* B **81** 094421
[33] Yoshida H, Takayama-Muromachi E and Isobe M 2011 *J. Phys. Soc. Japan* **80** 123703
[34] Matsuda M, de la Cruz C, Yoshida H, Isobe M and Fishman R S 2012 *Phys. Rev.* B **85** 144407
[35] Yoshida H, Isobe M and Takayama-Muromachi E 2010 *Abstracts of The 5th. Int. Conf. on Highly Frustrated Magnetism* W022
[36] Momma K and Izumi F 2011 *J. Appl. Crystallogr.* **44** 1272